International Symposium of Research Students on Material Science and Engineering
December 20-22, 2004, Chennai, India
Department of Metallurgical and Materials Engineering, Indian Institute of Technology Madras

THE ROLE OF SOLID SILICATES ON THE FORMATION OF GEOPOLYMERS DERIVED FROM COAL ASH

C. Rees, G.C. Lukey and J.S.J. van Deventer
Department of Chemical and Biomolecular Engineering,
The University of Melbourne, Victoria 3010, AUSTRALIA.

ABSTRACT

Geopolymers can be described as low calcium, alkali-activated, aluminosilicate cementitious binders. The further development and understanding of geopolymer technology is of significant interest because these advanced materials can be made cost-competitive to ordinary Portland cement (OPC), while exhibiting superior chemical and mechanical properties. The present study investigates the suitability of and structural characteristics of flyash-based geopolymers formed from different solid silicate industrial by-products. Results of the current work indicate that variations in geopolymer activator, while giving similar molecular bonding as shown by FTIR, display very different microstructures and therefore variations in macroscopic properties such as compressive strength. Factors identified that influence the microstructure and properties include trace elements and silicate solubility.

1. INTRODUCTION

A geopolymer can be described as a low calcium alkali activated aluminosilicate cement. The structure is comprised of predominantly Si-O-Al and Si-O-Si bonds arranged in a solid X-ray amorphous aluminosilicate network. The Al^{3+} is in IV-fold co-ordination and is charge balanced by an alkali cation such as K^+ or Na^+ [1]. The chemistry of geopolymers has often been equated to that of zeolites, since both have similar chemical compositions[1-3].

The further development and understanding of geopolymer technology is of significant commercial interest because these materials can be cost-competitive to ordinary Portland cement (OPC) and furthermore exhibit chemical and mechanical properties that are superior[4]. As shown previously in the literature, geopolymers can display high early strengths, and can be chemical and fire resistant[1]. Furthermore, the utilisation of industrial waste products, including coal ash and slags, as raw materials presents an opportunity for an environmentally friendly replacement for OPC. The further uptake of geopolymer technology has benefits of reducing landfill and prescribed waste, as well as Greenhouse gas emissions. The carbon dioxide (CO_2) emissions associated with the production of geopolymer cements can be as much as 10 times lower than OPC in terms of CO_2 emissions per unit volume of hardened concrete[5]. This represents the potential for a substantial reduction in world CO_2 emissions, since the cement industry is responsible for an estimated 5-10% of world CO_2 emissions[4,5].

The majority of studies conducted to date have used alkali silicate solutions for dissolution of raw materials to form the reactive precursors required for geopolymerisation[6]. It has been shown that silicate activation increases the dissolution of the starting materials and gives rise to favourable mechanical properties[7]. The use of silicate solutions for activation can cause rapid initial setting, which may not be beneficial in all potential applications of this material. Therefore the use of solid silicate materials is of interest because they could potentially

eliminate the need for an aqueous silicate source. This is expected to increase the commercial viability of geopolymeric materials because it enables the development of a 1-part mixture, similar to cement, which would allow more control of setting times and strength development profiles.

A proposed reaction model of geopolymerisation has been described previously[8], involving an OH^- promoted hydrolysis reaction (often referred to as alkali activation) followed by a condensation reaction of the hydroxylated species to form an inorganic polymer. During the condensation reaction, the soluble silicates react with soluble aluminate species to form an aluminosilicate gel. The gel then undergoes a solid-state transformation to form the final hardened binder[8]. In a system using a silicate solution, the silicate species are already in hydroxylated form (≡Si-OH), thereby are in a reactive form. However, when a solid silicate is used, silicate species must first be dissolved from the solid source by reaction with alkali and water, leading to a more gradual release of silica to the geopolymer gel. This can potentially give greater control over the characteristics of the gel by controlling the rate of silicate release, which can be manipulated by altering the silicate solubility. It is expected that a greater control over setting time and mechanical properties will result. Solid silicates obtained from many different sources, including various industrial by-products like rice hull ash and geothermal waste, are suitable for geopolymerisation.

Sustainable development necessitates renewable energy sources such as those derived from the combustion of agricultural residues, like rice hulls. World wide annual rice hull production is estimated at 80 million tonnes[9]. The utilisation of these energy sources produces large amounts of residual ash which can be high in amorphous silica. Another energy source not reliant on fossil fuels is geothermal energy. The production of geothermal power results in large amounts of residual silica, frequently removed as scale build up in pipes[10]. At the Cerro Prieto geothermal plant in Baja California, Mexico, total geothermal silica waste production is estimated to be 50,000tpa[11]. This material has no present use and is discarded to a waste pond with the threat of alkalisation of nearby agricultural lands due to overflow of high pH rainwater[12].

In the present study, both rich hull ash and geothermal silica waste are investigated to determine their effect on the structural characteristics and physical properties of flyash-based geopolymers. FTIR will be used to elucidate molecular structure, and SEM is used to examine the microstructure of geopolymers formed from each solid silicate source and flyash. These results will then be related to the compressive strength of each geopolymer.

2. EXPERIMENTAL PROCEDURES

2.1 Materials and Methods

The flyash (GFA) used originated from a coal-fired power station in Gladstone, Australia. The major oxide compositions are given in Table 1. Laboratory grade NaOH and distilled water was used to prepare alkaline solutions. Sodium silicate solution with $SiO_2/Na_2O = 2$ (PQ Australia) was used to prepare the silicate activated reference sample. Silica sand (effective size 0.5-0.6mm) was used to produce mortars for strength testing.

Geothermal silica scale was obtained from the Cerro Prieto Geothermal plant in Baja California, Mexico. The geothermal silica waste was scraped fresh from the pipes. The raw silica was washed with distilled water to remove salts and dried before use, as described previously[10]. Rice hull ash was obtained from Sunrice, Griffith, NSW, Australia. Two types of ash were tested, a

low carbon ash (LC) with 3% carbon and 95% silica, and a high carbon ash (HC) with 35% carbon and 62% silica[13].

All solid silicate materials used in the current work were ring milled, and had 100% of particles passing 106μm, with 50% passing 53μm. Each solid silicate was mixed with the GFA such that the effective Si/Al mole ratio was 2.2 (calculation of effective mole ratios exclude crystalline components in GFA[8]). The effective mole ratio of Al/Na = 0.85. The water to solids mass ratio used was 0.26 for all samples. The pastes were cured for 48 h at 40ºC in a sealed environment, and all analysis was performed within 7 days. Two reference samples were prepared: (1) a sample which was alkali activated and therefore had no secondary silicate source (effective Si/Al = 1.95); and (2) a sample that was prepared with sodium silicate solution such that the effective Si/Al = 2.2.

X-ray diffraction was performed on all samples using a Phillips PW 1800 diffractometer, coupled with a copper anode tube and a graphite monochromator. The CuK_α X-rays were generated at 30 mA and 40 kV to produce an average wavelength of 1.54184 Å. Scans were performed from 5 to 70° 2θ at 0.02° 2θ steps and integrated at the rate of 2 s $step^{-1}$. Scanning electron microscopy was performed using a Philips XL30 Field Emission Gun Scanning Electron Microscope (FEG-SEM). Fractured specimens were mounted on stubs and gold coated prior to analysis. Fourier-Transform Infrared (FTIR) spectra were obtained using a Bio-Rad FTS 165 FTIR spectrometer in transmittance mode, within the frequency range of 4000-400cm^{-1}. The samples were suspended in KBr plates. Spectra were obtained with a sensitivity of 4cm^{-1} with 8 scans per spectrum taken. Mortars for strength testing were prepared in polyethylene cube moulds with a side length of 5cm, using a weight ratio of silica sand to flyash of 2.1. Compressive strength testing was performed using an ELE compression machine with a loading rate of 0.9kN/s. Each reported strength was the average of 3 identical samples.

3. RESULTS AND DISCUSSION

Figure 1 shows the XRD diffractograms obtained for all cured geopolymer pastes and also the GFA raw material. The main crystalline phases identified in GFA are quartz (SiO_2) and mullite ($Al_6Si_2O_{13}$). GFA also consists of an X-ray amorphous aluminosilicate material, demonstrated by the broad hump from approximately 20 to 40º2θ[14]. It can be seen from Figure 1 that no significant change in intensity for the quartz or mullite peaks was observed in the geopolymer samples. This was expected, because it is predominantly the X-ray amorphous (glassy) phases in flyash that undergo dissolution and subsequent geopolymerisation at high pH[14].

A distinguishing feature between the AA reference sample (Si/Al = 1.95) and the other geopolymers (Si/Al = 2.2) is the formation of hydroxy sodalite[15], a low silica zeolite ($Na_6(Si_6Al_6O_{24}).8H_2O$). This is to be expected because the hydrothermal NaOH treatment of flyash is known to produce zeolites such as hydroxy sodalite[16]. It should be noted that the geothermal silica sample (GP) does show some small peaks in regions indicating minor sodalite formation. This could occur if the silica dissolved slowly and the silicate species in solution did not migrate far from the particle surface. This results in regions which are silica rich and others which are silica deficient. It is possible that the silica deficient gel is able to form the low silica crystalline hydroxy sodalite phase, while the X-ray amorphous phase with higher silicate content binds the phase separated system. The HC geopolymer shows a small hump in the region 20-25° 2θ. A hump in this region is characteristic of amorphous silica[17]. This indicates that there may be some unreacted rice hull ash in the HC system.

In general, the X-ray diffractograms for all silicate activated geopolymers were similar (Figure 1). Other than those mentioned above, no new crystalline phases were identified as products of

the reactions. Although XRD is an analytical technique commonly used to investigate geopolymer systems, the technique has significant limitations due to the apparent amorphous nature of geopolymer materials. The XRD diffractograms show that the raw materials and most of the newly formed geopolymer products are X-ray amorphous. For this reason, other analytical techniques need to be used in conjunction with XRD to provide insight into the structural characteristics of geopolymers.

SEM was performed on all geopolymers to investigate the microstructure. Figures 2 and 3 show the SEM micrographs for the alkali activated (AA) (no secondary silicate added) and the alkali silicate solution (LIQ) activated reference samples respectively. It can be seen that the AA sample (Figure 2B) has a much greater proportion of undissolved flyash particles than the LIQ geopolymer (Figure 3B). It is known that when alkali activation of flyash occurs in the absence of high concentrations of soluble silicate, dissolution is inhabited by the precipitation of secondary phases on the surface of flyash particles[7]. This surface precipitation is evident in Figure 2B. Similar phenomenon has also been demonstrated by other workers[3], along with the higher porosity observed when flyash is alkali activated in the absence of a secondary silicate source (Figure 2).

By comparing Figures 2A and 3A it can be seen that the AA geopolymer and the LIQ geopolymer both have different gel microstructures. In particular, the surface topography is quite varied; this is likely to be due to the absence and presence of silicates in the activating solution, altering the dissolution and precipitation reaction pathways. Figures 2A shows the AA sample has much smaller and more spherical particulates, while the LIQ sample has a more interconnected gel network with a continuous phase binding unreacted particles together[3] (Figure 3B). These results show that the amount of soluble silica in the system has an effect on the gel microstructure. The effect of these differences in microstructure on final mechanical properties of the geopolymers will be discussed later.

The SEM micrograph of the geopolymer formed using geothermal silica (GP) is presented in Figure 4. Comparing Figure 4 with Figure 3, it can be seen that the GP sample has a more porous structure than the LIQ geopolymer, which indicates that the solid silicate did not fully dissolve prior to gel formation. If rapid dissolution had occurred, the resulting microstructure would be expected to be more continuous and homogeneous[3]. Given that the GP sample has a more interconnected gel network than the AA sample (Figure 2), it is thought that partial dissolution of the geothermal waste has occurred, which contributed soluble silicate species to the system which may then react with hydroxylated aluminosilicate species (from the flyash) to form the aluminosilicate gel. This reaction process is expected to continue over time.

Comparing Figures 5 and 6, it is shown that the low carbon rice hull ash geopolymer (LC) has a significantly different topology than the high carbon rice hull ash gel (HC). This result is expected as the LC solid silicate is approximately 95% pure amorphous silica, whilst the HC solid contains 35% carbon[13]. It is unknown however at this stage whether the unusual gel microstructure (Figure 5A) is an aluminosilicate gel or a condensed silica phase. Figures 5B and 6B further indicate that the LC rice hull ash reacted to a greater extent than the high carbon ash. This observation is supported by the XRD results discussed previously, which indicated amorphous silica in this sample. The HC solid silicate is 35% carbon, the hydrophobicity of which may reduce the wettability of the particles and decrease the solubility of the silica. Lack of soluble silica would give a binder which resembles surface precipitation as seen in the AA sample (Figure 2); this is demonstrated by Figure 6B.

Activating with silicate solution doses the system with a high initial silicate concentration which will react rapidly with the glassy phase of the GFA. However, when a solid silicate is used, the initial concentration of silica in solution is low, and the solid can potentially dose the gel

constantly with new aqueous silica, maintaining the concentration of soluble silicates to a sufficient level as the reaction progresses. Since the gel microstructure has been seen to be greatly influenced by the soluble silicate concentration, it is expected that the solid silicate geopolymers will have a microstructure differing from the silicate solution activated reference. This is demonstrated by the electron micrographs in Figures 4-6.

It is expected that the solubility of the solid silicate source will control the rate at which the gel is dosed with silicate. Factors such as particle size, silica hydration will all affect the solubility and these parameters can be manipulated to provide greater control over the gelation reactions and potentially tailor the system for specific applications to produce a binder of optimal properties. Another factor influencing the microstructure is the presence of impurities. Various levels of impurities are present in all the waste silicates, including heavy metals. It is known that geothermal waters contain elements such as Br, Cr, Pb, Mn, Rb, Sr and Zn[18]; these will be present in trace amounts in the geothermal silica precipitate. Trace amounts of Mn, Ti, P, Pb, Cd, Cu and Zn are also present in the rice hull ashes[13]. These impurities may have a templating effect on gel development. It has been found previously that the most important influences on the effect of silica source on the zeolite crystallisation are the levels of soluble impurities and insoluble particulates smaller than 0.1μm in size[19]. Altering these factors leads to different zeolitic microstructures[19]. It is possible that trace metals and other impurities may effect the microstructure development of geopolymers (Figures 4-6), though this is outside the scope of the current work.

The structure and bonding of geopolymer samples was investigated by Fourier Transform infrared spectroscopy. The obtained FTIR spectra of cured geopolymer pastes and unreacted GFA are shown in Figure 7. Peaks associated with amorphous silica appear at around 1100cm^{-1}, 800cm^{-1} and 480cm^{-1}, these peaks correspond respectively to the stretching, bending and rocking of the Si-O-Si bond[20]. Although not shown, these peaks also appear in the spectra of each solid silicate raw material[17, 21].

As shown in Figure 7B, the peak at 800 cm^{-1} is of a lower intensity for all geopolymer samples, compared to the GFA raw material. This indicates that silica in both solid raw materials has reacted to some extent to form the geopolymer. It is important to note that this peak corresponds to a symmetric stretch and therefore is less intense using FTIR than the other (asymmetric) silicate peaks. The FTIR spectra of all geopolymer samples show a shoulder at approximately 1090cm^{-1}. This region corresponds to the strongest peak in the unreacted GFA spectra and is therefore thought to be due to unreacted GFA present in the geopolymers. From Figure 7C, it can be seen that the sample activated with silicate solution (LIQ) has the least intense shoulder at 1090cm^{-1}. This may be attributed to the LIQ activator adding a high concentration of silicate in solution at the mixing and initial hydrolysation reaction stages, aiding the dissolution of the GFA. It is known that high concentrations of both sodium and soluble silicates are required to completely hydrolyse the aluminosilicate raw material[8].

The peak at 1090cm^{-1} (most intense for GFA) is indicative of silicate stretching and it shifts after reaction. Following the hydrolysation of the raw materials, a structural reorganisation occurs in which aluminium ions are incorporated into the SiO_4 tetrahedra, forming the Si-O-Al network. The aluminium acts as a perturbation of silicate stretching vibrations as metal cations in other silicates do, such as sodium[22]. The extent of the peak shift has been found previously to correlate with the amount of aluminium incorporated into the silicate structure, when the alkali content is kept constant[23, 24]. Furthermore, the addition of alkali, forming non-bridging oxygens of the form Si-O$^-$ Na$^+$, causes a lowering of the molecular vibration force constant and therefore shifting of the peak associated with the asymmetric stretching of Si-O-Si(Al) bond to lower wavenumbers[8]. The extent of the peak shift has been found to be linear with alkali inclusion[8]. The peak shift for each geopolymer is show in Table 2.

The samples demonstrating the greatest shift of the peak from 1090cm^{-1} to lower wavenumbers were the HC and AA samples. Both of these samples also displayed similar porous microstructures, characteristic of a low silica content binder[3]. This would occur for the HC sample if the silica was not leached out from the HC during the reaction. The absence of sufficient aqueous silicate activator is known to lead to a higher Al content and higher relative Na content in the gel[3], this is expected to have caused the larger peak shift seen in these samples[23].

From the literature[25], it has been established that peaks in the FTIR spectra of silicate glasses associated with the vibration of ring structures occur mainly in the region 780-500cm^{-1}. The new peaks seen in all geopolymer samples at around 700cm^{-1} have been attributed to the development of these ring structures, which are found in the structure of zeolites and glassy analogues of identical composition[23]. Apart from the varied peak shift mentioned above, geopolymer FTIR spectra appeared quite similar, indicating that all have similar bonding on a molecular level.

Mechanical strength of each geopolymer was also investigated in the present work. Compressive strengths for all geopolymer samples were measured after 48 h curing at 40ºC. It can be seen from Table 3 that the geopolymer activated with a high concentration of soluble silicate has the highest compressive strength. This was expected due to the low porosity and continuous nature of the microstructure shown by SEM (Figure 2), and with a high degree of GFA dissolution indicated by FTIR results (Figure 7). An unexpected result was the high strength of the sample with no secondary silicate (AA). While this geopolymer has a higher early strength than the solid silicate geopolymers, the later strength development is likely to be poor, as the precipitation of secondary aluminosilicate phases on the surface of the fly ash prevents further dissolution over time[7].

The geothermal silica sample (GP) was expected to exhibit a relatively high strength due to the extremely high surface area of the particles 24,000m^2/kg[26]. This allows a large area for the reactions to occur and is likely to lead to faster dissolution of the silica. The strength of the HC geopolymer was quite low; however this was expected because it is thought that a high dissolution of silica did not occur (as shown by XRD, SEM and FTIR results). The low strength of the LC geopolymer has been attributed to the unusual topology of the microstructure, as shown by SEM (Figure 5).

CONCLUSION

Results of the current work indicate that it is possible to use solid industrial waste materials, which are high in amorphous silica, as a replacement for alkaline silicate solutions conventionally utilised in geopolymer synthesis. Geopolymers were examined in this study using a variety of analytical techniques: XRD, SEM, FTIR and compressive strength testing. The XRD results showed evidence of hydroxysodalite in alkali activated fly ash; however, as expected most reaction products were X-ray amorphous. A peak shift in the FTIR spectra, in the region characteristic of the silicate stretching vibration at 1090cm^{-1}, was found to be greater for samples with lower reactive silica content. SEM results showed these samples had a more porous microstructure, with the precipitation of secondary phases on the outside of the fly ash particles, lacking a continuous binding phase. The high carbon rice hull ash was thought to have remained largely unreacted as it displayed a similar porous microstructure and identical FTIR peak shift to the geopolymer which was alkali activated in the absence of a secondary silicate. Differences in microstructure of all other geopolymer samples have been attributed to the various doses of silicate to the gel during reaction, caused by differing rates of dissolution of the solid silicates. The effect of trace impurities in the waste silica sources is also expected to have contributed to this microstructural variation. Strength was found to be linked to microstructure,

in particular the topology and porosity of the binder. The use of solid silicates can potentially enable the tailoring of geopolymer gels to specific applications, thereby increasing the commercial viability of geopolymers, as a replacement for OPC.

ACKNOWLEDGEMENTS

The financial support of the Particulate Fluids Processing Centre (a Special Research Centre of the Australian Research Council) is gratefully acknowledged. The supply of solid silicates from Simon Spiers (HullTech) and Lauren Y. Gomez-Zamorano is appreciated.

REFERENCES

1. Davidovits, J. Journal of Thermal Analysis and Calorimetry **37** (8) (1991) 1633.
2. Xu, H. and van Deventer, J. S. J. International Journal of Mineral Processing **59** (3) (2000) 247.
3. Palomo, A., Grutzeck, M. W. and Blanco, M. T. Cement and Concrete Research **29** (8) (1999) 1323.
4. Lukey, G. C., van Deventer, J.S.J. Drivers for the establishment of a geopolymer industry. Materials 2003 - Adaptive Materials for a Modern Society, Sydney, Australia, 1-3 October (2003).
5. Gartner, E. Cement and Concrete Research **34** (9) (2004) 1489.
6. Davidovits, J., Mineral Polymers and Methods of Making Them. US Patent 4,349,386 USA (1982)
7. Lee, W. K. W. and van Deventer, J. S. J. Colloids and Surfaces A: Physicochemical and Engineering Aspects **211** (1) (2002) 49.
8. Lee, W. K. W. and van Deventer, J. S. J. Langmuir **19** (21) (2003) 8726.
9. Armesto, L., Bahillo, A., Veijonen, K., Cabanillas, A. and Otero, J. Biomass and Bioenergy **23** (3) (2002) 171.
10. Rincon, J. M. Journal of Thermal Analysis and Calorimetry **56** (1) (1999) 1261.
11. Gómez-Zamorano, L. Y., Escalante-García, J. I., Mendoza-Suárez, G. Journal of Materials Science **39** (12) (2004) 4021.
12. Diaz, C., Valle-Fuentes, F.J. American Ceramic Society Bulletin **78** (8) (1999) 112.
13. Spiers, S.Rice hull ash - Typical analysis Sunrice. Grifith,(2003).
14. Phair, J. W. and van Deventer, J. S. J. International Journal of Mineral Processing **66** (1-4) (2002) 121.
15. Murayama, N., Yamamoto, H. and Shibata, J. International Journal of Mineral Processing **64** (1) (2002) 1.
16. Poole, C., Prijatama, H. and Rice, N. M. Minerals Engineering **13** (8-9) (2000) 831.
17. Liou, T. Materials Science and Engineering A **364** (1-2) (2004) 313.
18. Diaz, C. and Rincon, J. M. Caracterización de la escoria de sílice de la planta geotérmica de Cerro Prieto. Congreso de la Soc. Española de Cerámica y Vidrio, España, (1989).
19. Hamilton, K. E., Coker, E. N., Sacco, A. J., Dixon, A. G. and Thompson, R. W. Zeolites **13** (8) (1993) 645.
20. Handke, M. and Mozgawa, W. Vibrational Spectroscopy **5** (1) (1993) 75.
21. Trujillo, G. C. D., Caracterizacion Y Purificacion del Residuo de Silice de la Central Geotermica de Cerro Prieto, Instituto de Ceramica y Vidrio (CSIC), (1994) 121.
22. Stoch, A., Paluszkiewicz, C., Gibala, T. and Bolek, A. Journal of Molecular Structure **293** (1993) 287.
23. Mozgawa, W., Sitarz, M. and Rokita, M. Journal of Molecular Structure **511-512** (1999) 251.
24. Chao, K., Shy, D., Sheu, S. and Lin, C. Microporous Materials **2** (2) (1994) 91.

25. Sitarz, M., Mozgawa, W. and Handke, M. Journal of Molecular Structure **404** (1-2) (1997) 193.
26. Escalante, J. I., Mendoza, G., Mancha, H., Lopez, J. and Vargas, G. Cement and Concrete Research **29** (4) (1999) 623.

TABLES

Table 1. Composition of Gladstone flyash as determined by XRF (mass %).

SiO_2	Al_2O_3	Fe_2O_3	CaO	MgO	TiO_2	LOI	Other
43.9	28.4	13.3	5.0	1.7	1.6	4.6	1.5

Table 2. Shifts of 1090cm^{-1} silicate peak in the FTIR spectra of all geopolymer samples.

Silicate activator	AA Ref	LIQ Ref	GP	LC	HC
Peak shift	101cm^{-1}	91cm^{-1}	93cm^{-1}	92cm^{-1}	101cm^{-1}

Table 3. Compressive strengths (σ, MPa) and bulk density (ρ, kg/m³) for geopolymer mortars.

Sample	LIQ Ref	AA Ref	GP	LC	HC
σ (MPa)	22.0	18.9	14.0	8.3	11.8
ρ (kg/m³)	2348	2356	2299	2348	2312

FIGURES

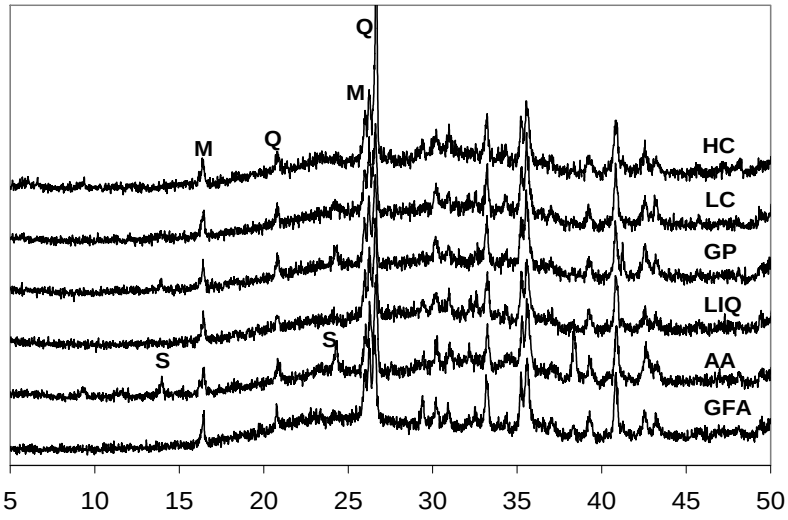

Figure 1. XRD diffractograms of geopolymers derived from flyash and solid silicate material: GP - geothermal silica, LC - low carbon rice hull ash, HC - high carbon rice hull ash. Reference samples: LIQ - silicate solution; AA – alkali activation only. GFA - unreacted flyash; S - hydroxy sodalite; Q - quartz; M – Mullite.

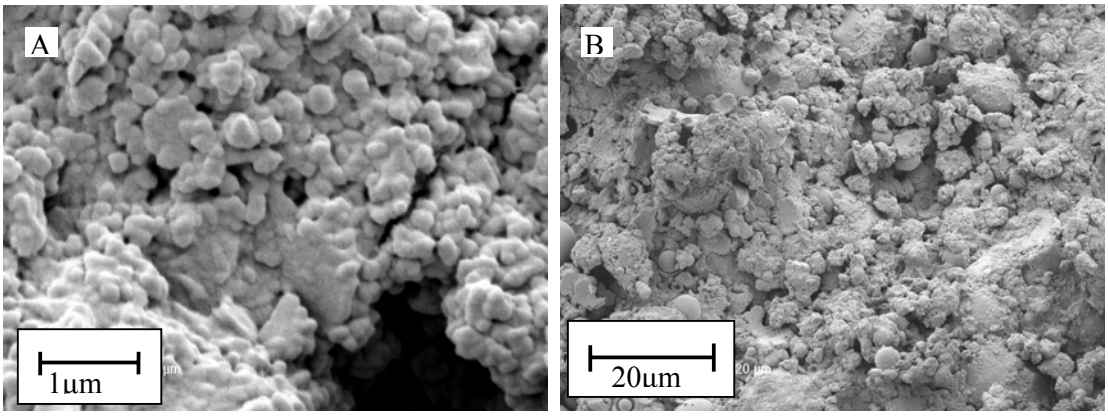

Figure 2. Electron micrographs of the alkali activated geopolymer (reference, AA).

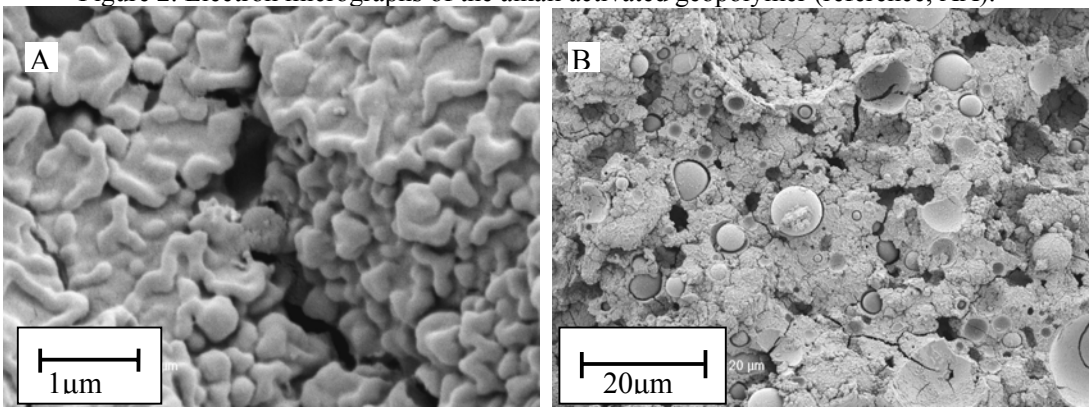

Figure 3. Electron micrographs of the soluble silicate activated geopolymer (reference, LIQ).

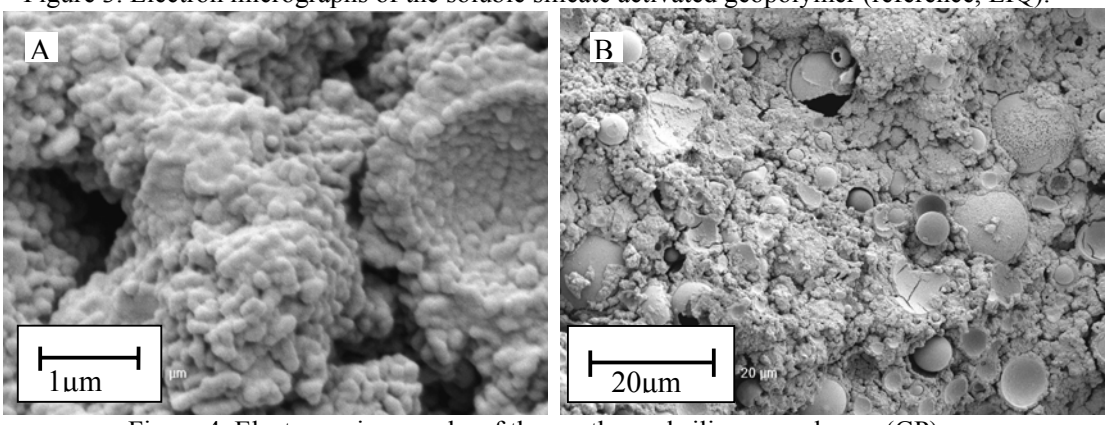

Figure 4. Electron micrographs of the geothermal silica geopolymer (GP).

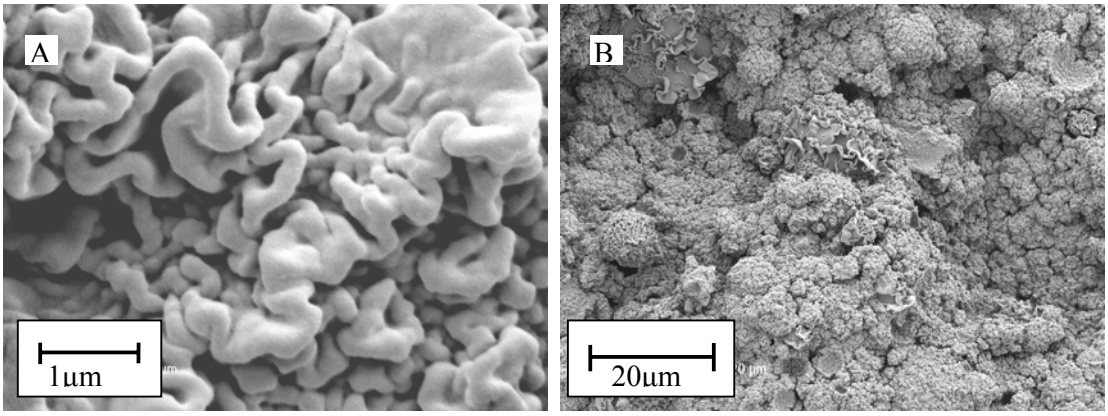

Figure 5. Electron micrographs of the low carbon containing rice hull ash geopolymer (LC).

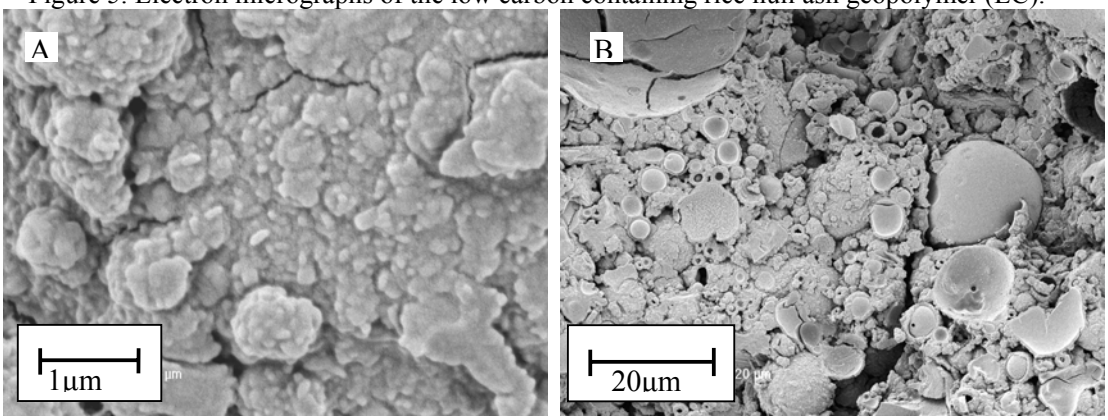

Figure 6. Electron micrographs of the high carbon containing rice hull ash geopolymer (HC).

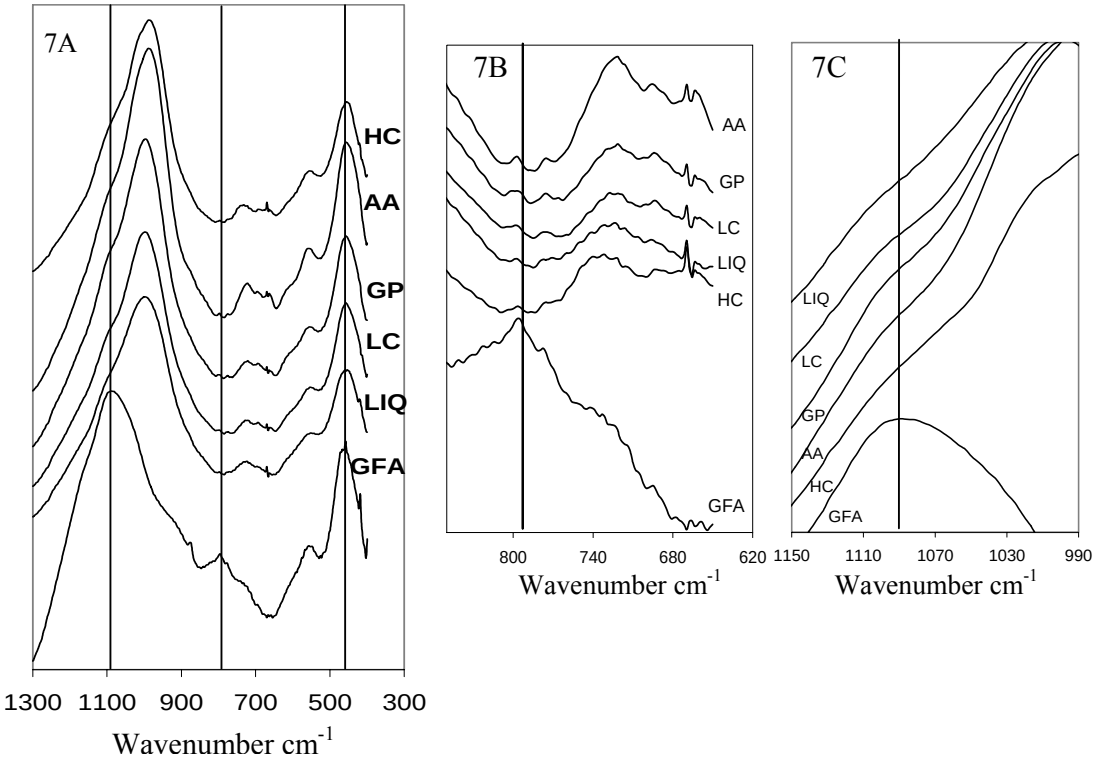

Figure 7. A - FTIR spectra for geopolymers and GFA raw material. B and C - Enlarged parts of the FTIR spectra for the geopolymers and GFA raw material.